Dalton Transactions

Accepted Manuscript

ROYAL SOCIETY OF CHEMISTRY

www.rsc.org/dalton

Cite this: DOI: 10.1039/c0xx00000x

www.rsc.org/xxxxxx

ARTICLE TYPE

Three Mn(II) Coordination Polymers with a Bispyridyl-based Quinolinate Ligand: the Anion-Controlled Tunable Structural and Magnetic Properties

Guozan Yuan[a,]*, Weilong Shan[a], Bin Liu[a], Lulu Rong[a], Liyan Zhang[b], Xianwen Wei[a,]*

Received (in XXX, XXX) Xth XXXXXXXXX 200X, Accepted Xth XXXXXXXXX 200X
DOI: 10.1039/b000000x

Three new Mn(II) coordination polymers, namely $[Mn_3L_6{\cdot}2H_2O]$ (**1**), $[MnL_2]$ (**2**), and $[MnL_2{\cdot}2H_2O]$ (**3**), were prepared by solvothermal reactions of Mn(II) salts with a bispyridyl-based quinolinate ligand. All complexes were characterized by elemental analysis, IR spectra, powder and single-crystal X-ray crystallography. Single crystal X-ray studies show that these coordination polymers exhibit an structural diversification due to the different counteranions (OAc^-, Cl^-, and NO_3^-). Complex **1** has a 2D supramolecular structure with a cyclic tetramer Mn_3L_6 secondary building units. Complex **2** possesses a rhombohedral grid network containing a kind of *meso*-helical chains (P+M) constructed via the metal-ligand coordination interactions. Complex **3** features a 3D non-porous structure based on the derangement of 2D grids. Magnetic susceptibility measurements indicate that the three Mn(II) polymers **1**-**3** show disparate magnetic properties due to their different supramolecular strutures.

Introduction

The design and construction of coordination polymers based on organic functional ligand are of significance not only for their intriguing variety of architectures and topologies but also for their tremendous potential applications in nonlinear optics, catalysis, gas adsorption, luminescence, magnetism, and medicine.[1-4] Numerous reports in this field have mainly focused on the design and preparation, as well as the structure-property relationships. Significant development has been achieved;[5-7] However, it is still a great challenge to rationally prepare and predict the desired products with exact structures and predefined properties. The resulting structures are determined by several factors, including the inbeing of the central metal ions[8], the predesigned organic ligands[9], solvents[10], metal-ligand ratio[11], pH value of solution[12], counterions[13], and so on.

Pyridine derivatives, either as the parent units or as higher oligomers (bipyridine, terpyridine, etc.), are very often utlized as appropriate building blocks to be incorporated in ligands[14]. Especially 2,2'-bipyridine (bipy) is frequently found in forming functional complexes, because it can form highly stable entities with metal ions[15]. In contrast to the neutral 2,2'-bipyridine, catecholate ligands possess a charge of 2-, and therefore address another kind of metal ions. The latter ligand unit recently have, in particular, attracted a lot of attention[16]. Interestingly, 8-hydroxyquinolinate (in its deprotonated form) is monoanionic and bridges the gap between the neutral bipyridine and the dianionic catecholate because it possesses one pyridine donor of bipy and one phenolate unit of catecholate. On the other hand, the geometry and chelating size of 8-hydroxyquinolinate are the same as found for bipy and catecholate[17]. It has been demonstrated that the 8-hydroxyquinoline unit is an ideal building block in coordination and supramolecular chemistry[18].With few notable exceptions, 8-hydroxyquinolinate-based coordination polymer with desirable structure and functionality has not yet been developed.[19]

Of particular interest to us are works on the elegant design and synthesis of novel quinolinate-based coordination polymers whose structures can be tuned by a careful selection of appropriate ligands and metals. Our goal is to achieve control over the molecular or supramolecular structures and thereby the physical properties of the new materials. In this study, we have synthesized a bispyridyl-based quinolinate ligand from the commercial available 8-hydroxyquinaldine to form Mn(II) coordination polymers and characterized the resulting polymers by microanalysis, IR, and powder and single-crystal X-ray diffraction. The polymer skeletons exhibit an structural diversification and fabricate one 2D supramolecular structure with a cyclic tetramer Mn_3L_6 secondary building units, one rhombohedral grid network, and one 3D non-porous structure in response to the counteranions OAc^-, Cl^-, and NO^{3-}, respectively. As a result, the three Mn(II) polymers exhibit disparate magnetic properties due to their different supramolecular strutures.

Results and discussion

Synthetic Chemistry

The ligand L-MOM (MOM: Methoxymethyl) was synthesized in 96% yield by Suzuki coupling reaction between 4-pyridylboronic acid and 5,7-dibromo-2-methyl-8-methoxymethoxyquinoline, which was obtained in two steps in excellent overall yield from the cheap commercial available 8-hydroxyquinaldine (Scheme 1).

The L-MOM ligand was fully characterized by ^{1}H and ^{13}C NMR, ESI-MS, and single-crystal X-ray diffraction. Single crystals of $[Mn_3L_6{\cdot}2H_2O]$ (**1**), $[MnL_2]$ (**2**) and $[MnL_2{\cdot}2H_2O]$ (**3**) were readily obtained in good yields by heating the corresponding Manganese(II) salts and L-MOM in water and methanol (or isopropanol). The -MOM group was completely removed from the starting ligands upon complexation with the metal ions. Complexes **1-3** are stable in air and insoluble in water and organic solvents, and were formulated on the basis of microanalysis, IR, and single-crystal X-ray diffraction. The reaction was originally accomplished in a 1:2 molar ratio of Mn(II) and L-MOM, but the products were not significantly affected by a change of the molar ratio. Moreover, when ethanol was used as a solvent instead of methanol or isopropanol, the same products were obtained. The complexes **1-3** are thus favorable species irrespective of the reactant molar ratios as well as the organic solvents used.

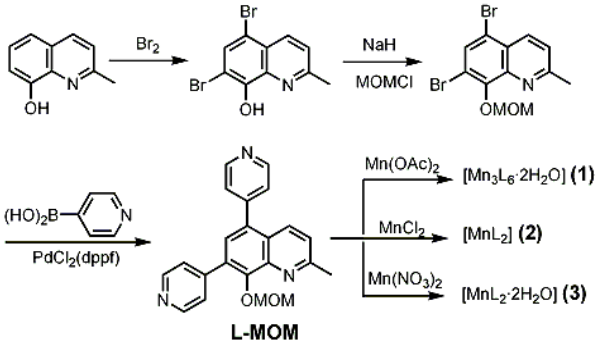

Scheme 1 Synthesis of ligand L-MOM and polymers **1-3**

Structural description

Ligand (L-MOM). Neutral ligand L-MOM was crystallographically characterized. The dihedral angle (ca. 37.1-55.3°) between the quinoline and pyridine moieties indicates that the molecule is noncoplanar. In the crystal structure of L-MOM, as shown in Fig 1a. there are intramolecular hydrogen bonds between the C-H groups of pyridine (or MOM) and the quinoline N (or O) atoms [C(2)···N(1) = 2.962(6) Å, C(24)···N(4) = 3.092(5) Å and C(14)···O(2) = 2.915(5) Å], and intermolecular hydrogen bonds between the MOM C–H group and pyridine nitrogen atoms [C(24)···N(3) = 3.514(5) Å]. It is notable that two independent molecules are held together by two intermolecular C-H···π interactions between C-H group of quinoline (or MOM) and pyridine ring of adjacent ligand (C-H···π: 3.707(6)-3.922(6) Å). By the coactions of above intermolecular noncovalent interactions, the structure extends to a 2D supramolecular structure in the bc plane (Fig. 1b).

$[Mn_3L_6{\cdot}2H_2O]$ (**1**). Single crystals of complex **1** was readily obtained in good yields by heating $Mn(OAc)_2$ and HL a mixture of MeOH and water. Complex **1** crystallizes in the monoclinic space group $P2_1/n$ with $Z = 2$. The asymmetry unit contains one half of a formula unit, that is, 1.5 Mn(II) atoms, three ligands HL, and one water molecule. As shown in Fig 2a, The Mn1 atom is six-coordinated by four nitrogen and two oxygen atoms provided by four ligands L, forming a octahedral geometry. The equatorial plane is occupied by two NO donors set of two L ligands around the Mn1 atom and the apical position by two pyridyl atoms of two other ligands. Mn2 atom is surrounded by three N and two O

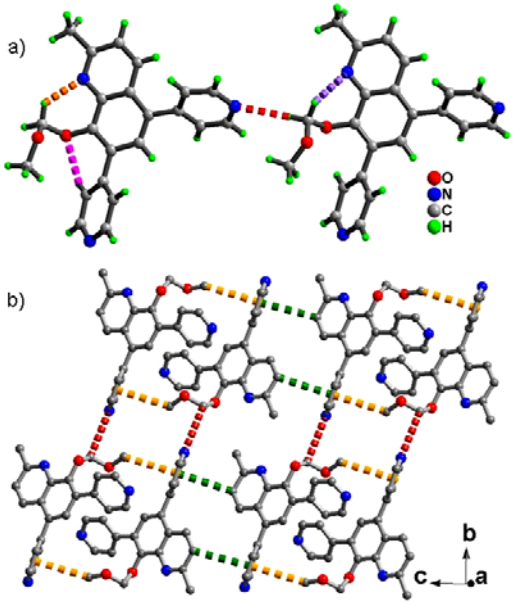

Fig. 1 (a) Perspective views of hydrogen-bonding interactions in L-MOM; (b) Perspective views of the 2D supramolecular structure fabricated by intermolecular noncovalent forces in L-MOM.

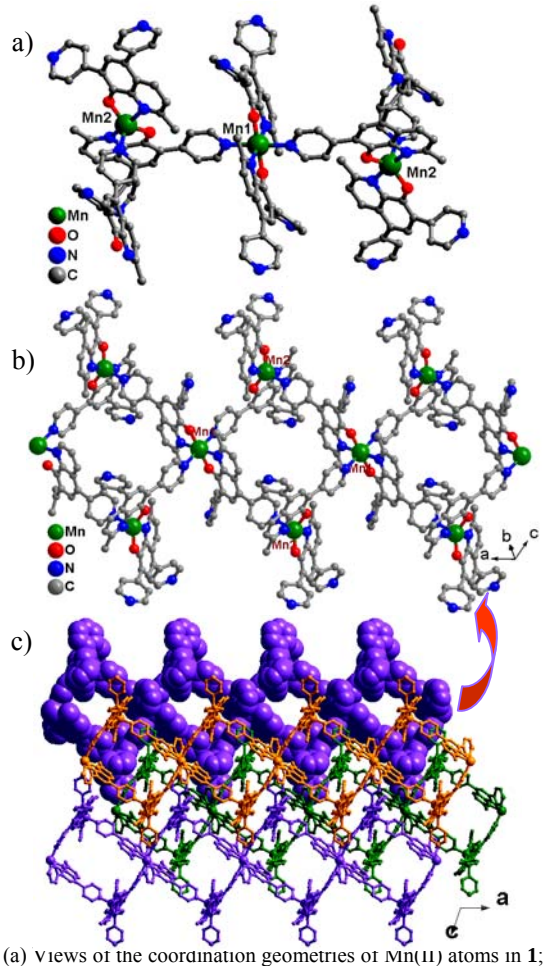

Fig. 2 (a) Views of the coordination geometries of Mn(II) atoms in **1**; (b) One 1D infinite chain in **1** along the *a*-axis; (c) 3-fold interpenetrated architecture in **1**.

atoms provided by three different L ligands, resulting in a distorted trigonal bipyramidal geometry with the equatorial plane occupied by the three atoms of three ligands and the apical position by two phenol oxygen atoms. The bond lengths and angels around Mn are 2.090(9)–2.260(6) Å for Mn–N, 1.940(6) and 2.039(5) Å for Mn–O, 136.3(3)º and 180.0(3)º for O–Mn–O, 77.7(3)–116.5(3)º for O–Mn–N, and 86.2(2)–180.0(1)º for N–Mn–N, respectively.

In complex **1**, six L ligands with eight uncoordinated pyridyl groups connect four Mn cations to form a cyclic tetramer Mn_4L_6, which is further linked into a 2D supramolecular structure in the *ac* plane (Fig 2b). Because of the spacious nature of 2D supramolecular structure, it allows another two independent identical structures to penetrate it in a normal mode, thus giving a 3-fold interpenetrated architecture (Fig 2c and S3). Interestingly, a helical chain is alternately arranged through the intermolecular C–H···π interactions (between C-H group of quinoline units and pyridine ring of adjacent ligand, 3.875(17) Å) in complex **1**. The helical chain is thus generated around the crystallographic 2(1) axis with a pitch of 23.721(15) Å, which is equal to the *b* axis length (Fig 2c).

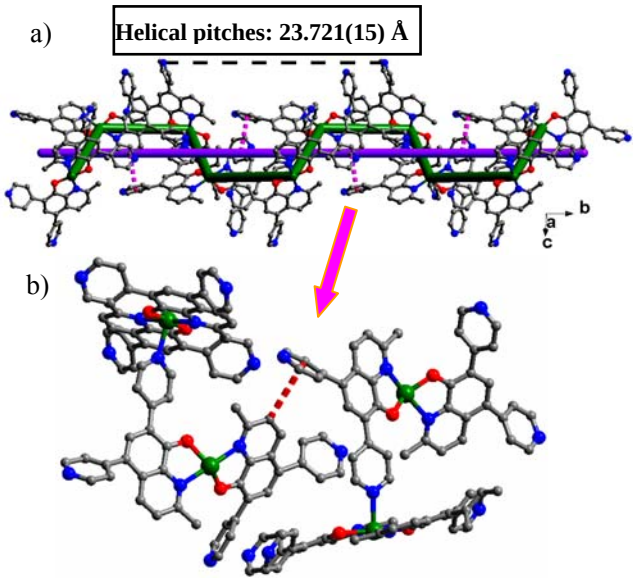

Fig. 3 (a) View of 1D helical chains fabricated via C–H···π interactions interaction in **1** along the *b*-axis; (b) Perspective views of intermolecular C-H···π interaction in **1**.

[MnL_2] (**2**). When the ligand L-MOM reacted with $MnCl_2$ under the same reaction conditions, the complex **2** was obtained as yellow block-like crystals. A single-crystal X-ray diffraction study of **2** reveals an infinite square grid consisting of six-coordinate Mn centers and bridging ligands (Fig 4a). **2** crystallizes in the monoclinic space group $P2_1/c$, with one half of a formula unit in the asymmetric unit, that is, 1/2 crystallographically independent Mn(II) atom and one ligand L. The coordination environment of Mn^{2+} ion in complex **2** is shown in Figure 4a, and it can be seen that Mn1 is six-coordinated to two phenolato oxygen atoms and four nitrogen atoms from four ligands L. The Mn(II) center adopts a octahedral geometry with the equatorial plane occupied by two chelating NO donor sets from two ligands L and the apical position by two nitrogen atoms of two other ligands.

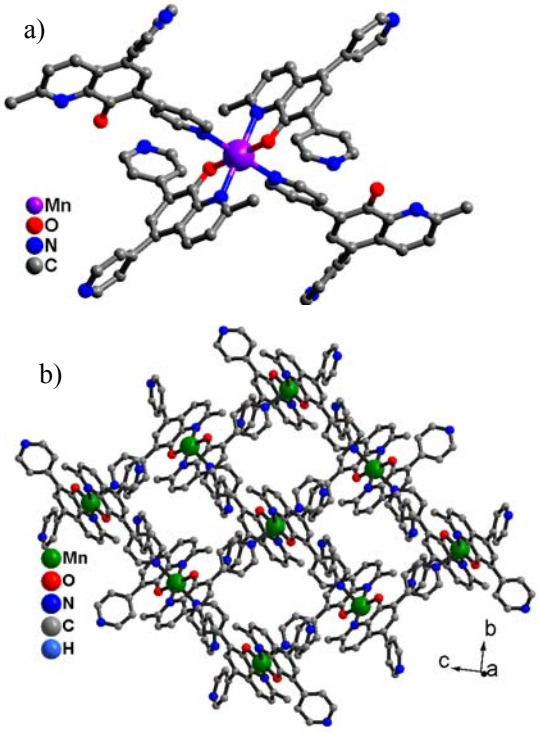

Fig. 4 (a) Views of the coordination geometries of Mn(II) atoms in **2**; (b) the rhombohedral grid structure of **2** in the *bc* plane.

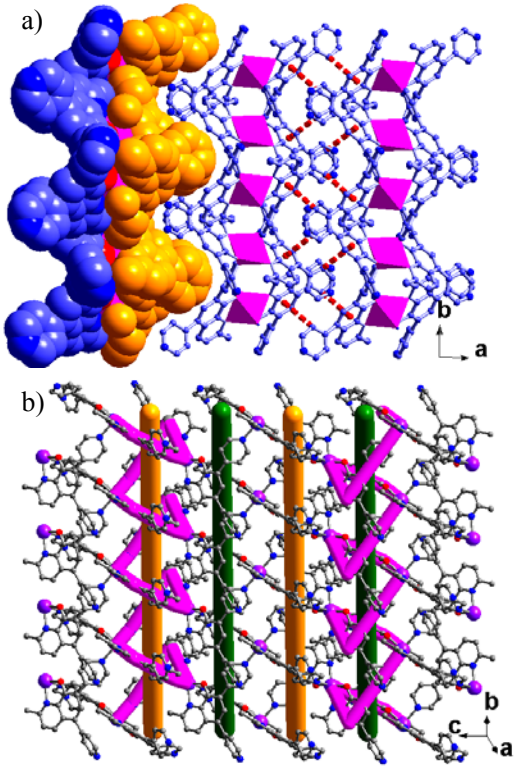

Fig. 5 (a) The 3D framework structure of **2** mediated by C–H···π interactions; (b) 2D layer structure of **2** containing *meso*-helical chains (P+M).

In the *bc* plane, each Mn1 atom is linked to four ajacent Mn1 atoms through the chelating NO donors and pyridyl groups of ligands L to form a rhombohedral grid structure (Fig 4b). These

grids are further linked by the C–H···π (between C-H group of pyridine and phenolato ring of adjacent ligand, 3.586(8) Å) interactions along the *a* axis to form a 3D porous framework structure (Fig 5a and S6). It is notable that a kind of *meso*-helical chains (P+M) constructed via the metal-ligand coordination interactions are observed in the solid state of this compound (Fig 5b). These *meso*-helical chains with a pitch of 10.2952(14) Å are alternately arranged along *b* axis, which is identical to the *b* axis length. To the best of our knowledge, such supramolecular layer containing *meso*-helical chains is very rare.

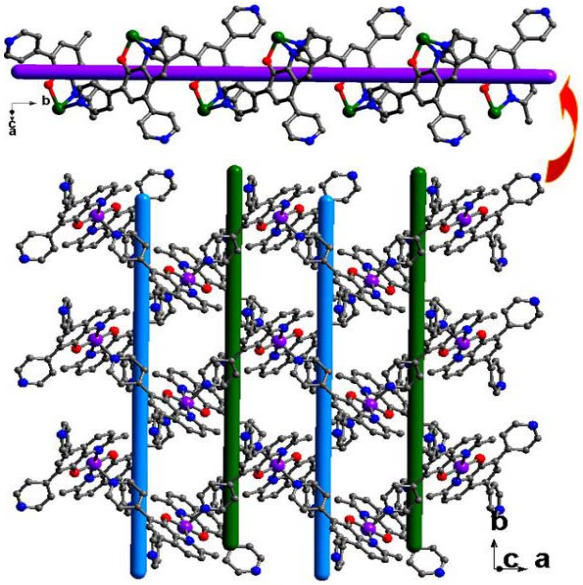

Fig. 6 The meso-helical chains in **3** are alternately arranged in the *ab* plane.

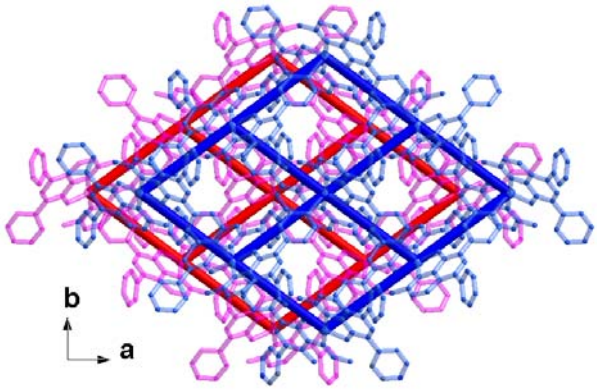

Fig. 7 The twofold interpenetrated architecture in **3**.

$[MnL_2{\cdot}2H_2O]$ (**3**). In order to further investigate the influence of counterions on the formation and structures of the complexes, ligand L-MOM reacted with $Mn(NO_3)_2$ under the same conditions, complex **3** ($MnL_2{\cdot}2H_2O$) was obtained. Single-crystal X-ray diffraction analysis reveals that the complex **3** crystallizes in the orthorhombic system, space group $Pca2_1$. As shown in Fig. S6, there are one crystallographically independent Mn(II) atom, two L ligand, and two water molecules in the asymmetric unit. As compared with the structure of **2**, the linkage of MnL remains intact, but L ligands in **3** undergo significant twists around metal centers, as indicated by the dihedral angles between the terminal pyridyl ring in the 7- position and phenolato ring decreasing from 42.26º in **2** to 38.89º and 37.42º in **3**. Similar to **2**, The terminal pyridyl groups in the 7- position and chelating NO donors of ligands link the Mn(II) centers into a 2D grid structure in the *ab* plane, and the distances between Mn centers exhibits a subtle distinction (**2**, 8.8332(25) Å; **3**, 8.7862(11) Å and 8.8517(12) Å). A kind of *meso*-helical chain (P+M) are alternately arranged in the *ab* plane (Fig 6). Note that complex **3** avoids extremely large void space by the derangement of 2D grids. (Fig 7 and S9).

PXRD and Fluorescent Properties

To prove that the crystal structures of complexes **1-3** are truly representative of their bulk materials, powder X-ray diffraction (PXRD) experiments (Fig 8) were carried out on the as-synthesized samples. The peak positions of experimental and simulated PXRD patterns are in good agreement, which confirm their phase purity. The difference in intensity of some diffraction peaks may be attributed to the preferred orientation of the crystalline samples.

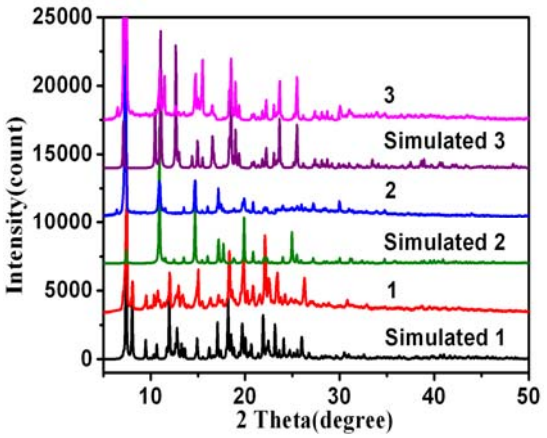

Fig. 8 PXRD patterns of complexes **1-3**.

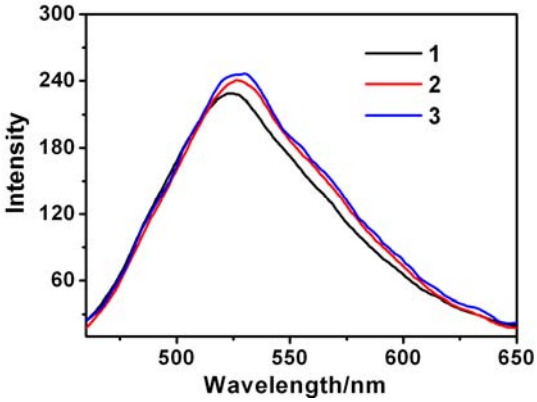

Fig. 9 Emission spectra of complexes **1-3** in the solid state.

The fluorescent properties of complexes **1-3** and their corresponding free L-MOM ligand were investigated in the solid state at room temperature (Fig 9). **1-3** exhibit intense photoluminescences with the emission maximum at 523, 527, and 527 nm, respectively, upon excitation at 365 nm. Compared with the bond at 402 nm of L-MOM ligand, complexes exhibit remarkable red shift. However, the green emissions of complexes

1-**3** show no significant difference, and may originate from metal-to-ligand charge transfer (MLCT) transition.

Magnetic Properties

The magnetic measurements were performed on polycrystalline samples of **1**, **2** and **3** using a SQUID magnetometer under an applied field of 1000 Oe over the temperature range 2-300 K. Fig.10 shows the $\chi_M T$ and χ_M^{-1} vs. T plots of compound **1**. The magnitude of $\chi_M T$ at 300 K is 6.02 cm^3 K mol^{-1}, which is slightly higher than the spin only value of 4.375 cm^3 K mol^{-1} for uncoupled high spin Mn(II) (S = 5/2) based g = 2.00. With the temperature decreasing, the $\chi_M T$ values decrease with a very slow speed and attain a minimum of 4.74 cm^3 K mol^{-1} at ca. 47 K. Then the $\chi_M T$ values start to increase with a high speed and reach the highest peak with the value of 8.47 cm^3 K mol^{-1} at 31 K, strongly suggesting the presence of global antiferromagnetic interactions and three-dimensional magnetic ordering[21]. After that, the $\chi_M T$ values decrease abruptly to the minimum value 4.11 cm^3 K mol^{-1}, at 2 K, probably due to the interlayer antiferromagnetic interaction . The magnetic suscetibility conform to Curie–Weiss law in a range of 30-300K and give the nagative constant θ = −16.54 K, Curie constant C = 6.08 cm^3 K mol^{-1}, further conforming the antiferromagnetic couping nature between the Mn(II) ions.

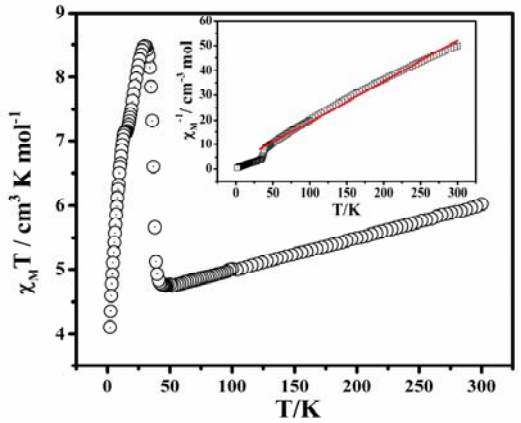

Fig.10 Temperature dependence of magnetic susceptibility in the form of $\chi_M T$ *vs*. T for 1, inset: χ_M^{-1} *vs*. T plot for **1** (open circles and red line represent experimental data and fits).

The $\chi_M T$ and χ_M^{-1} vs. T plots for compound **2** as shown in Fig. 11. The $\chi_M T$ value per Mn(II) at 300 K is about 6.20 cm^3 K mol^{-1}, which is slightly higher than the spin only value of 4.375 cm^3 K mol^{-1} for uncoupled high spin Mn(II) (g = 2.00 and S =5/2). and it gradually decreases to 5.58 cm^3 K mol^{-1} at 41K. Upon further cooling, $\chi_M T$ increases dramatically and reaches a maximum of 6.26 cm^3 K mol^{-1} at 31 K. The Curie–Weiss fit of the data above 30 K gives C = 6.14 cm^3 mol^{-1} K and θ = −3.02 K. The negative value of the Weiss constant reveals the antiferromagnetic interactions between Mn(II) ions. Below 30 K, the $\chi_M T$ drops quickly and approaches a value of 5.26 cm^3 mol^{-1} K at 2 K. The further decrease may be due to the saturation effect[22].

As shown in Fig. 12, compound **3**, at room temperature the value of product $\chi_M T$ is 4.44 cm^3 K mol^{-1}, which is similar to the expected value of 4.375 cm^3 K mol^{-1} for one isolated high-spin Mn(II) ion (g = 2.00 and S =5/2). Upon cooling, the χ_MT value decreases continuously, reaching a value of 2.64 cm^3 K mol^{-1} at 2 K. These features indicate an antiferromagnetic coupling. Data fitting of the χ_M^{-1}–T curve using the Curie–Weiss law gives the Curie constant (C = 4.41 cm^3 K mol^{-1}) and the Weiss constant (θ = −3.07 K). The negative θ value suggesting an antiferromagnetic interaction between Mn(II) ions in compound **3**.

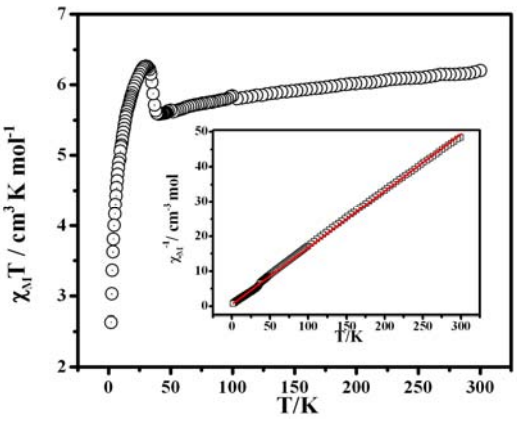

Fig. 11 Temperature dependence of magnetic susceptibility in the form of $\chi_M T$ *vs*. T for **2**, inset: χ_M^{-1} *vs*. T plot for **2** (open circles and red line represent experimental data and fits).

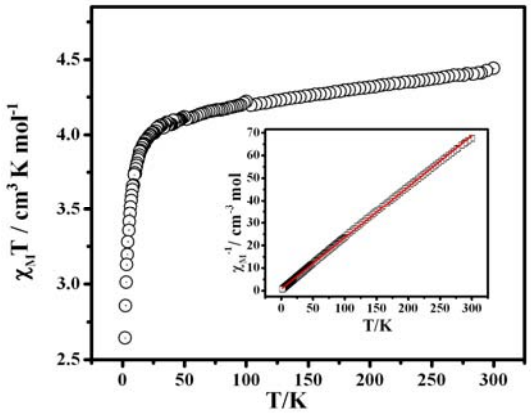

Fig.12 Temperature dependence of magnetic susceptibility in the form of $\chi_M T$ *vs*. T for **3**, inset: χ_M^{-1} *vs*. T plot for **3** (open circles and red line represent experimental data and fits).

Experimental

Materials and characterization methods

All of the chemicals are commercial available, and used without further purification. Elemental analyses of C, H and N were performed with an EA1110 CHNS-0 CE elemental analyzer. The IR (KBr pellet) spectrum was recorded (400-4000 cm^{-1} region) on a Nicolet Magna 750 FT-IR spectrometer. Powder X-ray diffraction (PXRD) data were collected on a DMAX2500 diffractometer using Cu Kα radiation. The calculated PXRD patterns were produced using the SHELXTL-XPOW program and single crystal reflection data. All fluorescence measurements were carried out on a LS 50B Luminescence Spectrometer (Perkin Elmer, Inc., USA). ^{1}H and ^{13}C NMR experiments were carried out on a MERCURY plus 400 spectrometer operating at resonance frequencies of 100.63 MHz. Electrospray ionization mass spectra (ES-MS) were recorded on a Finnigan LCQ mass

spectrometerusing dichloromethane-methanol as mobile phase. Variable temperature magnetic measurements were carried out on a Quantum Design SQUID MPMS XL-7 instrument (2−300 K) in the magnetic field of 1 kOe, and the diamagnetic corrections were evaluated using Pascals constants.

Synthesis of L-MOM and 1-3

5,7-dibromo-2-methyl-8-hydroxyquinoline[20]. To a solution of 8-hydroxyquinaldine (3.18 g, 20 mmol) in MeOH (30 mL) was added solid $NaHCO_3$ (3.18 g, 37.8 mmol). To this suspension was added drop-wise (5 min) at rt a solution of Br_2 (3.2 mL, 62.4 mmol, excess) in methanol (10 mL). The reaction mixture was stirred at rt for 30 min to give orange solution and white precipitate. Solid Na_2SO_3 (23.0 g, 183.0 mmol, excess) was added to this suspension in small portions over 5 min to quench residual Br_2. The reaction was mildly exothermic. A colorless suspension was obtained after final addition and further stirring for 30 min. It was diluted with water (40 mL) to give thick white suspension which was stirred for 30 min. The pH of reaction mixture at that stage was close to neutral (pH test paper). The product was filtered, thoroughly washed with water and extracted with CH_2Cl_2/water to remove inorganic materials. Organic layer was evaporated to give the product as pale orange solid (6.0 g, 96%).

Synthesis of 5,7-dibromo-2-methyl-8-methoxymethoxyquinoline**.** Under a nitrogen atmosphere, the solution of 5,7-dibromo-2-methyl-8-hydroxyquinoline (3.15 g, 10.0 mmol) in THF (30 mL) was added to a suspension of NaH (1.0 g, 41.7 mol) in anhydrous THF (30 mL) at 0 °C with stirring. The resulting solution was stirred at 0 °C for 30 min, and then methoxymethyl chloride (2.7 mL, 35.8 mmol) was slowly added. The mixture was allowed to warm to room temperature and stirred for 12 h. Then the reaction was quenched by water. After separation, the aqueous layer was extracted with CH_2Cl_2 (3×60

Table 1 Crystal data and structure refinement for Ligand L-MOM, complexes **1-3**.

Identification code	**L-MOM**	**1**	**2**	**3**
Empirical formula	$C_{22}H_{19}N_3O_2$	$C_{120}H_{88}Mn_3N_{18}O_8$	$C_{40}H_{28}N_6O_2Mn$	$C_{40}H_{32}N_6O_4Mn$
Formula weight	357.40	2074.90	679.62	711.62
Temperature (K)	141(2)	173(2)	141(2) K	173(2)
Wavelength (Å)	0.71073	0.71073	0.71073	1.54178
Crystal system	Monoclinic	Monoclinic	Monoclinic	Orthorhombic
Space group	$P2_1/n$	$P2_1/n$	$P2_1/c$	$Pca2_1$
Unit cell dimensions	a = 12.619(3) Å	a = 14.623(11) Å	a = 13.073(5) Å	a = 14.1579(9) Å
	b = 21.772(7) Å	b = 23.721(16) Å	b = 10.287(4) Å	b = 10.5162(7) Å
	c = 14.394(4) Å	c = 15.965(11) Å	c = 14.362(6) Å	c = 24.8704(15) Å
	alpha = 90º	alpha = 90º	alpha = 90º	alpha = 90º
	beta = 110.5º	beta = 109.0º	beta = 114.2º	beta = 90º
	gamma = 90º	gamma = 90º	gamma = 90º	gamma = 90º
Volume (Å^3), Z	3705.1(18), 8	5238(6), 2	1762.1(12), 2	3703.4(4), 4
Density (calculated) (Mg/m^3)	1.281	1.316	1.281	1.276
Absorption coefficient (mm^{-1})	0.084	0.424	0.418	3.291
F(000)	1504	2146	702	1468
θ range for data collection (º)	1.78 to 27.47	1.72 to 27.47	1.71 to 27.56	3.55 to 68.14
Reflections collected	13780	22778	7503	10405
Independent reflections	8295 [R(int) = 0.0483]	11394 [R(int) = 0.1123]	3964 [R(int) = 0.0528]	5705 [R(int) = 0.0465]
Completeness to theta	27.47/97.6%	25.24/98.0%	27.56/97.3 %	68.14/97.6%
Data / restraints / parameters	829 / 0 / 487	11394 / 130 / 700	3964 / 0 / 223	5705 / 1 / 444
Goodness-of-fit on F^2	1.026	0.909	0.950	1.033
Final R indices [I>2sigma(I)]	R_1 = 0.0683, wR_2 = 0.1780	R_1 = 0.0965, wR_2 = 0.2299	R_1 = 0.0485, wR_2 = 0.0945	R_1 = 0.0734, wR_2 = 0.2064
R indices (all data)	R_1 = 0.1576, wR_2 = 0.2532	R_1 = 0.2600, wR_2 = 0.3213	R_1 = 0.1243, wR_2 = 0.1205	R_1 = 0.0869, wR_2 = 0.2209
Largest diff. peak and hole (e.Å^{-3})	0.243 and -0.240	0.717 and -0.580	0.396 and -0.575	0.695 and -0.394

mL). The combined organic layers were washed with brine and dried over $MgSO_4$. After removal of the solvent, the residue was purified by column chromatography on silica gel (1:1, hexane-CH_2Cl_2) to afford 5,7-dibromo-2-methyl-8-methoxymethoxyquinoline as a white solid (3.09 g, 86%). ^{1}H NMR (400 MHz, $CDCl_3$) δ: 8.32 (d, J = 8.0 Hz, 1H), 7.90 (s, 1H), 7.37 (d, J = 8.0 Hz, 1H), 5.65 (s, 2H), 3.74 (s, 3H), 2.75 (s, 3H); ^{13}C NMR (400 MHz, $CDCl_3$) δ: 159.9, 150.3, 143.1, 136.2, 132.9, 126.6, 123.6, 116.4, 116.3, 100.4, 58.5, 25.6; ESI-MS: m/z 360.0 ($[M+1]^+$), 361.0 ($[M+2]^+$), 361.9 ($[M+3]^+$); Elemental analysis (%): calcd for ($C_{12}H_{11}Br_2NO_2$) C: 39.92, H: 3.07, N: 3.88; found C: 39.88, H: 3.16, N: 3.79.

Ligand L-MOM. 5,7-dipyridyl-2-methyl-8-methoxymethoxyquinoline (4.8 g, 13.4 mmol), 4-pyridylboronic acid (4.8 g, 40.11 mmol), Na_2CO_3 (7.0 g, 66.04 mmol) and $PdCl_2(dppf)\cdot CH_2Cl_2$ (0.41g, 0.80 mmol) were weighted into a 250 mL Schlenk flask, which was then pump-purged with N_2 three times. DME (60 mL) and H_2O (30 mL) were added under a dry N_2 atmosphere. The mixture was stirred at 95 °C for overnight. The reaction mixture was cooled to room temperature and extracted with CH_2Cl_2. The organic layers were dried over anhydrous Na_2SO_4 and then concentrated under reduced pressure. The crude product was purified by column chromatography on silica gel (8:3:1 AcOEt-hexane-Et_3N) to afford ligand L-MOM as a white solid. Yield: 4.4 g, 92%. ^{1}H NMR (400 MHz, $CDCl_3$) δ: 8.72 (dd, J = 1.6, 4.4 Hz, 2H), 8.69 (dd, J = 1.6, 4.4 Hz, 2H), 8.05 (d, J = 8.8 Hz, 1H), 7.63 (dd, J = 1.6, 4.4 Hz, 2H), 7.42 (s, 1H), 7.38 (dd, J = 1.6, 4.4 Hz, 2H), 7.30 (d, J = 8.8 Hz, 1H), 5.43 (s, 2H), 3.06 (s, 3H), 2.76 (s, 3H); ^{13}C NMR (400 MHz, $CDCl_3$) δ: 159.4, 150.4, 150.3, 150.0, 147.1, 146.2, 142.5, 134.1, 133.6, 131.6, 127.7, 125.9, 125.1, 124.9, 123.3, 100.5, 57.5, 25.8; ESI-MS: m/z 358.1($[M+1]^+$), 359.0 ($[M+2]^+$). Elemental analysis (%): calcd for ($C_{22}H_{19}N_3O_2$) C: 73.93, H: 5.36, N: 11.76 (%); found C: 73.82, H: 35.31, N: 11.83.

Synthesis of complexes **1-3**. A mixture of MnX_2 (X = OAc^-, Cl^-, NO_3^-, 0.02 mmol), L-MOM (0.04 mmol), H_2O (0.2 mL), and MeOH (2 mL) in a capped vial was heated at 80 °C for one day. Yellow blocklike crystals of **1-3** suitable for single-crystal X-ray diffraction were collected, washed with ether and dried in air. The products were not significantly affected by a change in the molar ratio of Mn(II) and L-MOM (1:1, 2:1 or 1:2). Yield: **1**, 10.8 mg, 78%; **2**, 10.9 mg, 80%; **3**, 11.6 mg, 81%.

Elemental Analysis data and IR of [$Mn_3L_6\cdot 2H_2O$] (**1**): Anal (%). Calcd for $C_{120}H_{88}N_{18}O_8Mn_3$: C, 69.46; H, 4.27; N, 12.15. Found: C, 69.32; H, 4.36; N, 12.08. FTIR (KBr pellet): 3443.6(s), 1743.5(w), 1597.0(s), 1550.1(s), 1515.3(s), 1414.5(s), 1384.2(s), 1376.2(s), 1335.6(m), 1320.7(m), 1276.0(m), 1218.8(w), 1109.3(m), 1027.4(m), 1003.5(w), 833.8(m), 802.8(w), 760.3(w), 746.5(w), 657.6(m), 584.8(m), 513.0(m), 471.7(m).

Elemental Analysis data and IR of [MnL_2] (**2**): Anal (%). Calcd for $C_{40}H_{28}N_6O_2Mn$: C, 70.69; H, 4.15; N, 12.37. Found: C, 70.50; H, 4.22; N, 13.32. FTIR (KBr pellet): 3445.2(s), 1595.3(s), 1543.9(s), 1513.7(s), 1439.7(s), 1421.0(s), 1384.4(s), 1366.16(s), 1332.6(m), 1275.1(m), 1218.6(w), 1184.7(w), 1106.26(m), 1068.1(w), 1006.6(m), 833.8(m), 804.49(w), 758.0(w), 744.9(w), 722.5(w), 683.0(w), 655.9(w), 584.4(m), 511.4(w).

Elemental Analysis data and IR of [$MnL_2\cdot 2H_2O$] (**3**): Anal (%). Calcd for $C_{40}H_{32}N_6O_4Mn$: C, 67.13; H, 4.51; N, 11.74. Found: C, 67.05; H, 4.66; N, 13.85. FTIR (KBr pellet): 3443.2(s), 1595.6(s), 1544.2(s), 1513.5(s), 1439.7(s), 1420.8(s), 1384.5(s), 1365.8(s), 1332.8(m), 1275.1(s), 1217.8(w), 1184.7(w), 1106.3(m), 1067.9(w), 1006.2(m), 834.0(s), 804.4(w), 758.1 (m), 744.7(w), 721.9(m), 705.2(m), 683.1(m), 655.6(m), 584.4(s), 510.9(m), 457.8(m).

X-ray crystallography. Single-crystal XRD data for compounds L-MOM, **1 , 2** and **3** were all collected on a Bruker APEX area-detector X-ray diffractometer with Mo_{Ka} radiation (λ = 0.71073 Å) or Cu-Kα radiation (λ = 1.54178 Å). The empirical absorption correction was applied by using the SADABS program (G. M. Sheldrick, SADABS, program for empirical absorption correction of area detector data; University of Göttingen, Göttingen, Germany, 1996). The structure was solved using direct method, and refined by full-matrix least-squares on F^2 (G. M. Sheldrick, SHELXTL97, program for crystal structure refinement, University of Göttingen, Germany, 1997). Crystal data and details of the data collection are given in Table 1, whereas the selected bond distances and angles are presented in Table S1-3. The CCDC number of L-MOM, **1**, **2** and **3** are 972562, 972563, 972564, and 972565, respectively.

Conclusion

In summary, three Mn(II) coordination polymers with different structures are prepared under solvothermal conditions, using Mn(II) salts (different counteranions: OAc^-, Cl^-, and NO_3^-) and a bispyridyl-based quinolinate ligand synthesized from the cheap commercial available 8-hydroxyquinaldine. In the solid state, the polymers **1-3** show an structural diversification and fabricate one 2D supramolecular structure, one rhombohedral grid structure, and 3D non-porous structure in response to the counteranions OAc^-, Cl^-, and NO_3^-, respectively. On the other hand, the three supramolecular structures contain three kinds of helical chains because of different coordination and other non-covalent interactions in **1-3**. However, the three Mn(II) polymers exhibit disparate magnetic properties due to their different supramolecular strutures. These results further enrich our knowledge of structural topologies for coordination networks, and they also provide a useful strategy to tune the structures and properties for the design of new functional coordination polymers.

Acknowledgements

This work was financially supported by the National Natural Science Foundation of China (Nos. 21201002 and 21271006), Anhui Provincial Natural Science Foundation (1308085QB22). Provincial natural science research program of higher education institutions of Anhui province (KJ2013Z028), Anhui Provincial Science Foundation for Outstanding Young Talent (2012SQRL187), National Training Programs of Innovation and Entrepreneurship for Undergraduates (201210360087).

Notes and references

[a] *School of Chemistry and Chemical Engineering, Anhui University of Technology, Maanshan 243002, China. Fax: +86 555 2311552; Tel: +86 555 2311807;* [b] *School of Chemistry and Chemical Engineering, Huangshan University , Huangshan 245041, China. Tel: +86 13955996865; E-mail: yuanguozan@163.com (Guozan Yuan); xwwei@ahut.edu.cn (Xianwen Wei)*

† Electronic Supplementary Information (ESI) available: Additional structural figures, the selected bond distances and angles for L-MOM, **1**, **2** and **3** were included. CCDC 972562, 972563, 972564, and 972565. For ESI and crystallographic data in CIF or other electronic format see DOI: 10.1039/b000000x.

1 (a) M. O'Keeffe, O. M. Yaghi, *Chem. Rev.,* 2012, **112**, 657; (b) S. Horike, S. Shimomura, S. Kitagawa, *Nat. Chem.*, 2009, **1**, 695; (c) G. Férey, *Chem. Soc. Rev*., 2008, **37**, 191; (d) H. Wu, Q. Gong, D. H. Olson, J. Li, *Chem. Rev*., 2012, **112**, 836; (e) L. E. Kreno, K. Leong, O. K. Farha, M. Allendorf, R. P. V. Duyne, J. T. Hupp, *Chem. Rev*., 2012, **112**, 1105; (f) G. K. Kolea, J. J. Vittal, *Chem. Soc. Rev.,* 2013, **42**, 1755-1775.

2 (a) M. D. Allendorf, C. A. Bauer, R. K. Bhakta, R. J. T. Houk, *Chem. Soc. Rev*., 2009, **38**, 1330; (b) K. Sumida, D. L. Rogow, J. A. Mason, T. M. McDonald, E. D. Bloch, Z. R. Herm, T. Bae, J. R. Long, *Chem. Rev*., 2012, **112**, 724; (c) J. Li, R. J. Kuppler, H. Zhou, *Chem.Soc. Rev*., 2009, **38**, 1477; (d) J. A. Hurd, R. Vaidhyanathan, V. Thangadurai, C. I. Ratcliffe, I. L. Moudrakovski, G. K. H. Shimizu, *Nat. Chem*., 2009, **1**, 705; (e) S. M. Cohen, *Chem. Rev.,* 2011, **112**, 970; (f) Y. Cui, Y. Yue, G. Qian, B. Chen, *Chem. Rev*., 2012, **112**, 1126.

3 (a) L. Ma, C. Abney, W. Lin, *Chem. Soc. Rev*., 2009, **38**, 1248; (b) J.-Y. Lee, O. K. Farha, J. Roberts, K. A. Scheidt, S. T. Nguyen, J. T. Hupp, *Chem. Soc. Rev*., 2009, **38**, 1450; (c) Y. Liu, W. Xuan, Y. Cui, *Adv. Mater*., 2010, **22**, 4112; (d) W. Xuan, C. Zhu, Y. Liu, Y. Cui, *Chem. Soc. Rev.,* 2012, **41**, 1677; (e) C. Zhu, G. Yuan, X. Chen, Z. Yang, Y. Cui, *J. Am. Chem. Soc.,* 2012, **134**, 8058; (f) G. Li, W. Yu, Y. Cui, *J. Am. Chem. Soc.,* 2008, **130**, 4582.

4 (a) D. Weng, Z. Wang, S. Gao, *Chem. Soc. Rev.,* 2011, **40**, 3157; (b) E. Coronado, G. Mínguez Espallargas, *Chem. Soc. Rev*., 2013, **42**, 1525.

5 (a) K. L. Mulfort, O. K. Farha, C. L. Stern, A. A. Sarjeant, J. T. Hupp, *J. Am. Chem. Soc*., 2009, **131**, 3866; (b) J. Yang, A. Grzech, F. M. Mulder, T. J. Dingemans, *Chem. Commun*., 2011, **47**, 5244; (c) Y.-G. Lee, H. R. Moon, Y. E. Cheon, M. P. Suh, *Angew. Chem. Int. Ed*., 2008, **47**, 7741; (d) A. Lan, K. Li, H. Wu, D. H. Olson, T. J. Emge, W. Ki, M. Hong, J. Li, *Angew. Chem. Int. Ed.,* 2009, **48**, 2334; (e) Z. –J. Yao, W. –B. Yu, Y. –J. Lin, S. –L. Huang, Z. –H. Li, G. –X. Jin, *J. Am. Chem. Soc*., 2014, **136**, 2825; (f) H. Li, Y. –F. Han, Y. –J. Lin, Z. –W. Guo, G. –X. Jin, *J. Am. Chem. Soc*., 2014, **136**, 2982; (g) Y. –Y. Zhang, Y. –J. Lin, G. –X. Jin, *Chem. Commun*., 2014, **50**, 2327; (h) S. –L. Huang, Y. –J. Lin, T. S. A. Hor, G. –X. Jin, *J. Am. Chem. Soc*., 2013, **135**, 8125; (i) S. –L. Huang, A. –Q. Jia, G. –X. Jin, *Chem. Comm*., 2013, **49**, 2403.

6 (a) S. Zheng, X. Zhao, S. Lau, A. Fuhr, P. Feng, X. Bu, *J. Am. Chem. Soc*., 2013, **135**, 10270; (b) J. E. Mondloch, W. Bury, D. Fairen-Jimenez, S. Kwon, E. J. DeMarco, M. H. Weston, A. A. Sarjeant, S. T. Nguyen, P. C. Stair, R. Q. Snurr, O. K. Farha, J. T. Hupp, *J. Am. Chem. Soc.,* 2013, **135**, 10294; (c) W. M. Bloch, R. Babarao, M. R. Hill, C. J. Doonan, C. J. Sumby, *J. Am. Chem. Soc.,* 2013, **135**, 10441; (d) X. Rao, T. Song, J. Gao, Y. Cui, Y. Yang, C. Wu, B. Chen, G. Qian, *J. Am. Chem. Soc.,* 2013, **135**, 15559; (e) H. -L. Jiang, D. Feng, K. Wang, Z. -Y. Gu, Z. Wei, Y. –P. Chen, H. –C. Zhou, *J. Am. Chem. Soc*., 2013, **135**, 13934; (f) Z. Wei, W. Lu, H. –L. Jiang, H. –C. Zhou, *Inorg. Chem.,* 2013, **52**, 1164.

7 (a) H. Reinsch, M. Krüger, J. Marrot, N. Stock, *Inorg. Chem.,* 2013, **52**, 1854; (b) Z. Lin, Y. Huang, T. Liu, X. Li, R. Cao, *Inorg. Chem.,* 2013, **52**, 3127; (c) Q. Tang, S. Liu, Y. Liu, J. Miao, S. Li, L. Zhang, Z. Shi, Z. Zheng, *Inorg. Chem.,* 2013, **52**, 2799; (d) B. A. Blight, R. Guillet-Nicolas, F. Kleitz, R. Wang, S. Wang, *Inorg. Chem.,* 2013, **52**, 1673. (e) Y. –F. Han, W. –G. Jia, W. –B. Yu, G. –X. Jin, *Chem. Soc. Rev*., 2009, 3419; (f) Y. –F. Han, W. –G. Jia, Y. –J. Lin, G. –X. Jin, *Angew. Chem. Int. Ed*., 2009, **48**, 6234; (g) Y. –F. Han, H. Li, G. –X. Jin, *Chem. Commun*., 2010, **46**, 6879; (h) Y. –F. Han, Y. –J. Lin, G. –X. Jin, *Dalton Trans.,* 2011, **40**, 10370.

8 (a) M. Du, X. J. Jiang, X. J. Zhao, *Chem. Commun.,* 2005, 5521; (b) M. R. Montney, S. M. Krishnan, R. M. Supkowski, R. L. LaDuca, *Inorg. Chem.,* 2007, **46**, 7362; (c) B. Xu, Z. Lin, L. Han, R. Cao, *CrystEngComm*., 2011, **13**, 440; (d) J. Yang, J. F. Ma, S. R. Batten, Z. M. Su, *Chem. Commun*., 2008, 2233; (e) J. Q. Liu, Y. Y. Wang, Y. N. Zhang, P. Liu, Q. Z. Shi, S. R. Batten, *Eur. J. Inorg. Chem.,* 2009, 147; (f) Y. Y. Liu, J. F. Ma, J. Yang, J. C. Ma, G. J. Ping, *CrystEngComm.,* 2008, **10**, 565.

9 (a) K. Kasai, M. Sato, *Chem.-Asian J.,* 2006**,** **1**, 344; (b) N. N. Adarsh, P. Dastidar, *Cryst. Growth Des.,* 2010, **10**, 483; (c) L. Hou, W. J. Shi, Y. Y. Wang, B. Liu, W. H. Huang, Q. Z. Shi, *CrystEngComm.,* 2010, **12**, 4365; (d) H. J. Hao, D. Sun, F. J. Liu, R. B. Huang, L. S. Zheng, *Cryst. Growth Des.,* 2011, **11**, 5475; (e) Z. H. Zhang, S. C. Chen, J. L. Mi, M. Y. He, Q. Chen, M. Du, *Chem. Commun.,* 2010, **46**, 8427; (f) G. Yuan, C. Zhu, Y. Liu, W. Xuan, Y. Cui, *J. Am. Chem. Soc*., 2009, **131**, 10452; (g) G. Yuan, C. Zhu, Y. Liu, W. Xuan, Y. Cui, *Chem. Eur. J.,* 2009, **15**, 6428; (h) G. Yuan, C. Zhu, Y. Liu, Y. Cui, *Chem. Commun.,* 2011, **47**, 3180-3182.

10 (a) W. H. Zhang, Y. L. Song, Y. Zhang, J. P. Lang, *Cryst. Growth Des.,* 2008, **8**, 253; (*b*) Y. Chen, H. X. Li, D. Liu, L. L. Liu, N. Y. Li, H. Y. Ye, Y. Zhang, J. P. Lang, *Cryst. Growth Des*., 2008, **8**, 3810; (*c*) M. L. Tong, S. L. Zheng, X. M. Chen, *Chem. Eur. J.,* 2000, **6**, 3729; (*d*) M. F. Wang, X. J. Hong, Q. G. Zhan, H. G. Jin, Y. T. Liu, Z. P. Zheng, S. H. Xu, Y. P. Cai, *Dalton Trans.,* 2012, **41**, 11898.

11 (a) Y. P. Wu, D. S. Li, F. Fu, W. W. Dong, J. Zhao, K. Zou, Y. Y. Wang, *Cryst. Growth Des.,* 2011, **11**, 3850; (b) X. J. Luan, X. H. Cai, Y. Y. Wang, D. S. Li, C. J. Wang, P. Liu, H. M. Hu, Q. Z. Shi, S. M. Peng, *Chem.-Eur. J*., 2006, **12**, 6281; (c) P. P. Liu, A. L. Cheng, Q. Yue, N. Liu, W. W. Sun, E. Q. Gao, *Cryst. Growth Des*., 2008, **8**, 1668; (d) L. Carlucci, G. Ciani, S. Maggini, D. Proserpio, M. *Cryst. Growth Des.,* 2008, **8**, 162.

12 (a) P. Q. Zheng, Y. P. Ren, L. S. Long, R. B. Huang, L. S. Zheng, *Inorg. Chem.,* 2005, 44, 1190; (b) X. L. Wang, C. Qin, E. B. Wang, Y. G. Li, Z. M. Su, L. Xu, L. Carlucci, *Angew. Chem. Int. Ed.*, 2005, **44**, 5824; (c) P. X. Yin, J. Zhang, Z. J. Li, Y. Y. Qin, J. K. Cheng, L. Zhang, Q. P. Lin, Y. G. Yao, *Cryst. Growth Des.,* 2009, **9**, 4884; (d) H. C. Fang, J. Q. Zhu, L. J. Zhou, H. Y. Jia, S. S. Li, X. Gong, S. B. Li, Y. P. Cai, P. K. Thallapally, J. Liu, G. J. Exarhos, *Cryst. Growth Des.,* 2010, **10**, 3277.

13 (a) R. Custelcean, *Chem. Soc. Rev.,* 2010, **39**, 3675; (b) F. J. Liu, D. Sun, H. J. Hao, R. B. Huang, L. S. Zheng, *Cryst. Growth Des.,* 2012, **12**, 354; (c) Z. Q. Yu, M. Pan, J. J. Jiang, Z. M. Liu, C. Y. Su, *Cryst. Growth Des*., 2012, **12**, 2389; (d) R. Sekiya, M. Fukuda, R. Kuroda, *J. Am. Chem. Soc.,* 2012, **134**, 10987.

14 (a) S. Li, T. Xiao, C. Lin, L. Wang, *Chem. Soc. Rev.,* 2012, **41**, 5950; (b) E. C. Constable, *Tetrahedron.,* 1992, **48**, 10013.

15 (a) E. D. Bloch, D. Britt, C. Lee, C. J. Doonan, F. J. Uribe-Romo, H. Furukawa, J. R. Long, O. M. Yaghi, *J. Am. Chem. Soc.,* 2010, **132**, 14382; (b) S. Das, S. Karmakar, D. Saha, S. Baitalik, *Inorg. Chem.,* 2013, **52**, 6860; (c) S. Ladouceur, D. Fortin, E. Zysman-Colman, *Inorg. Chem.,* 2010, **49**, 5625; (d) Z. Li, E. Badaeva, A. Ugrinov, S. Kilina, W. Sun, *Inorg. Chem*., 2013, **52**, 7578.

16 (a) M. Albrecht, *Chem. Soc. Rev*., 1998, **27**, 81; (b) D. Caulder, K. N. Raymond, *J. Chem. Soc.,* 1999, 1185; (c) B. F. Abrahams, N. J. FitzGerald, R. Robson, *Inorg. Chem.,* 2010, **49**, 5953; (d) R. K. Totten, M. H. Weston, J. K. Park, O. K. Farha, J. T. Hupp, S. T. Nguyen, *ACS Catal.,* 2013, **3**, 1454.

17 M. Albrecht, M. Fiege, O. Osetska, *Coord. Chem. Rev*., 2008, **252**, 812.

18 (a) K. Sokołowski, I. Justyniak, W. Śliwiński, K. Sołtys, A. Tulewicz, A. Kornowicz, R. Moszyński, J. Lipkowski, J. Lewiński, *Chem. Eur. J*., 2012, **18**, 5637; (b) M. Czugler, R. Neumann, E. Weber, *Inorg. Chim. Acta.,* 2001, **313**, 100; (c) H. M. Colquhoun, D. J. Williams, Z. Zhu, *J. Am. Chem. Soc*., 2002, **124**, 13346.

19 (a) G. Yuan, Y. Huo, X. Nie, X. Fang, S. Zhu, *Tetrahedron* 2012, **68**, 8018; (b) G. Yuan, Y. Huo, L. Rong, X. Nie, X. Fang, *Inorg. Chem. Commun.,* 2012, **23**, 90; (c) G. Yuan, Y. Huo, X. Nie, H. Jiang, B. Liu, X. Fang, F. Zhao, *Dalton Trans.,* 2013, **42**, 2921; (d) G. Yuan, L. Rong, X. Qiao, L. Ma, X. Wei, *CrystEngComm.,* 2013, **15**, 7307.

20 N. M. Shavaleev, R. Scopelliti, F. Gumy, J. C. G. Bünzli, *Inorg. Chem.,* 2009, **48**, 2908.

21 (a) F. Dai, J. Dou, H. He, X. Zhao, D. Sun, *Inorg. Chem*., 2010, **49**, 4117; (b) D. Zhang, L. Zhang, H. Wang, Y. Chen, Z. Ni, J. Jiang, *Inorg. Chem. Commun.,* 2010, **13**, 895.

22 (a) X. Li, X. Wang, S. Gao, R. Cao, *Inorg. Chem*., 2006, **45**, 1508; (b) D. K. Rittenberg, K. Sugiura, Y. Sakata, S. Mikami, A. J. Epstein, J. S. Miller, *Adv.Mater*., 2000, **12**, 126; (c) K. Wang, X. Yi, X. Wang, X. Li, E. Gao, *Dalton Trans*., 2013, **42**, 8748.

Graphic Abstract

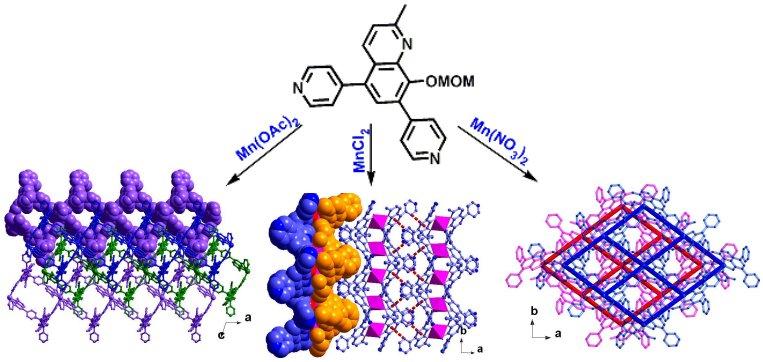

Three anion-controlled Mn(II) coordination polymers were assembled from a bispyridyl-based quinolinate ligand. They exhibit disparate magnetic properties due to their different supramolecular structures.